FTIR Study of Ageing Epoxy Resin Reinforced by Reactive Graphitic Nanofibers

Soumen Jana, Wei-Hong Zhong

Department of Mechanical Engineering and Applied Mechanics, North Dakota State University, Fargo, North Dakota 58105

Received 26 March 2007; accepted 2 May 2007
DOI 10.1002/app.26925
Published online 28 August 2007 in Wiley InterScience (www.interscience.wiley.com).

ABSTRACT: We previously developed a novel modified epoxy matrix for macrocomposites using reactive graphitic nanofibers (r-GNFs), which showed improved mechanical properties. This article is devoted to study the efficacy of the r-GNFs against the damage due to exposition of the matrix to hygrothermal environment and UV radiation. Moisture sorption characteristics of the pure epoxy and nanoepoxy were investigated and all kinds of matrices showed similar absorption behavior. Both diffusion and relaxation processes in sorption were observed. DSC curves of nonaged specimens of all concentrations confirmed that samples were not fully cured and r-GNFs lowered the curing degree. The effects of ageing were studied through the changes of molecular conformation by Fourier Transform infrared spectroscopy (FTIR). The results show that UV radiation assists in post-curing of the matrices. Hydroxyl unit, carbonyl unit, and epoxide unit were chosen to study the degradation. It is observed that the degradation due to UV radiation is more severe compared with that due to hygrothermal expose. It also reveals that r-GNFs resist the degradation of the epoxy resin; particularly, the nanoepoxy with 0.3 wt % of r-GNFs has the highest ageing resistance, which is in agreement with our previously tested results of mechanical properties. J Appl Polym Sci 106: 3555–3563, 2007

Key words: nanoparticle; epoxy resin; ageing; UV radiation; FTIR

INTRODUCTION

Epoxy resins are important matrices of composite materials for various engineering applications due to their low density, good thermal, physical, electrical, and mechanical properties, besides their good processability for making structural components.[1,2] Epoxy systems can be cured with anhydride and amide curing agents and in curing process there is no release of small molecules.[3] However, modification of epoxy is still necessary since some applications demand higher mechanical and thermal properties as well as stability under harsh conditions. Incorporation of various reinforced nanosized phases into epoxy-based materials is one of the ways to solve the problem with success.[4,5]

Different kinds of nanoparticles such as graphitic nanofibers (GNFs), carbon nanotubes (CNTs), nanoclays, polyhedral oligomeric silsesquioxanes (POSS), and nanosilica (Aerosil®) have been used to enhance the properties of epoxy resins.[6–9] GNFs have attractive mechanical and physical properties and low cost with high availability among these nanoparticles.[10,11] In addition, GNFs have graphene layer structures with edges, which can be utilized for functionalization with bi-functional linkers to promote covalent bonding between these GNFs and polymer resin molecules.[12,13] The mechanical properties of epoxy resin may be improved with GNFs as occurred to other thermosets,[14] thermoplastics.[15,16] However, many improvements come about with the nanofiber concentration ranging from about 5 wt % to as high as 20 wt %.[17–22] It is also reported that to obtain significant increase in mechanical properties and homogeneity, it is desirable to keep the concentration of nanofiber low (<5 wt %).

To enhance the properties, a kind of reactive nanofibers (r-GNFs) from functionalized herringbone GNFs with 3,4′-oxydianiline (GNF-ODA, Fig. 1) was produced.[12,23] This r-GNF has reactive hydrogen in its —OH— unit and the reactive hydrogen can react with epoxide groups in the curing reaction of epoxy resins as an amine type curing agent does. Thus, r-GNFs are then part of the matrix structure and both the epoxy and the r-GNFs form into a unified resin system instead of being ''a simple physical mixture or a usual nanocomposite.'' Therefore, it is called nanoepoxy, which is expected to be a matrix with high performance for macrocomposite materials.

The components for various applications made from epoxy resins may be exposed to humidity and

Correspondence to: W.-H. Zhong (katie.zhong@ndsu.edu).
Contract grant sponsor: NASA; contract grant number: NNM04AA62G.
Contract grant sponsor: NSF through NIRT; contract grant number: 0506531.

Journal of Applied Polymer Science, Vol. 106, 3555–3563 (2007)

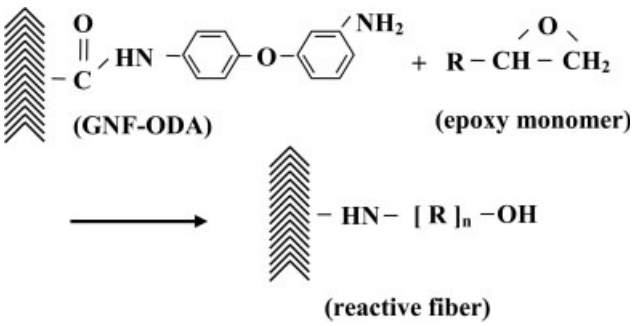

Figure 1 Formation of a reactive nanofiber (r-GNF).[23,24]

elevated temperatures. The mechanical and other properties of epoxy systems can be lowered due to moisture absorption. At elevated temperatures, the absorbed water generally works as plasticizer and thus lowers the mechanical performances.[24,25] Besides, bio-degradation of polymer materials, e.g., by fungal growth is likely to be increased with absorbed moisture in the materials even at ambient temperatures if porosity exists in the composite materials. Therefore, there is a need for understanding the changes in epoxy resins due to hygrothermal ageing. For outdoor applications, epoxy resins may be exposed to UV radiation and this may affect the mechanical properties of epoxy composites. It is reported that UV radiation causes generation of characteristic cracks in an epoxy resin coating.[26,27] Specially, amine cured epoxy resins show low strength, toughness and glass transition temperature due to gamma radiation and UV radiation. It is found that the radiations cause chain scissions, oxidization of exposed upper layer.[28]

We previously developed a novel modified epoxy matrix for macrocomposites using the reactive graphitic nanofibers (r-GNFs). Our previous experiments showed that r-GNFs help in improving mechanical properties of the nanoepoxy at both normal and ageing environments with moisture and UV irradiations. In this study, our main objective is to determine the aging mechanisms of the nanoepoxy and to find out why and how the r-GNFs may help in reducing the degradation of the nanoepoxy. Thus, hygrothermal aging and UV aging were conducted on the pure-epoxy and the nanoepoxy. FTIR analyses were performed to study the changes of molecular conformations in matrix specimens due to hygrothermal and UV aging.

EXPERIMENTS

Materials

Epoxy resin: Epon® 828 and cure agents: Epikure™ W were purchased from Miller–Stephenson Chemical Inc. Vanderbilt University supplied functionalized GNFs, GNF-ODA (Fig. 1). A reactive diluent from Sigma-Aldrich Co. was butyl glycidyl ether (BGE) with a similar epoxide unit as can be found in the epoxy resin, but the viscosity of the diluent is much lower as compared with the epoxy resin.

Matrix preparation

A mixture of GNF-ODA nanofibers and diluent (BEG) (1 : 50 by weight) was treated with sonication by a sonifier (Branson® 450) with power level 70 W for 3 h at the room temperature (25°C). Such a sonication treatment can reduce the length of the GNF-ODA nanofibers to 400–800 nm but it does not change the diameter of the nanofibers (25–100 nm). These small GNF-ODA nanofibers were allowed to react with BEG for 36 h, and thus, r-GNFs were obtained as shown in Figure 1.[12,23] The solution was then vacuumed in a hot vacuum chamber [120°C] to control the r-GNF/BGE ratio to 1 : 6 by weight.

The curing agent was added to the epoxy 828 in a ratio of 24 : 100 by weight. The pure epoxy matrix contained only the cure agent. Proper amounts of r-GNF/BGE solutions were added into the pure epoxy matrix to make the nanoepoxy matrices having 0.2, 0.3, and 0.5% r-GNFs loadings by weight. Low level sonication was conducted for each mixture for an hour at room temperature to disperse the r-GNFs into the matrix.

Sample preparation

Pure epoxy and nanoepoxy matrices with different r-GNF loadings were poured into molds separately, cured for 8 h at the temperature of 120°C (information source: Miller–Stephenson Chemical Inc., the company from which the epoxy resin and curing agent were purchased) and then cooled naturally to the room temperature. Each type of the cured matrices was cut into pieces and the surface of each piece was smoothened by polishing to obtain the specimens as described in Table I. Matrix specimens with different r-GNF contents (Epoxy: 0 wt %, *N*-6/2: 0.2 wt %, *N*-6/3: 0.3 wt %, and *N*-6/5: 0.5 wt %) were immersed into water for 30 days for hygrothermal aging tests and the water temperature was 60°C.

TABLE I
The Compositions of the Samples

Specimen group	Description of the matrix used	
	Materials	Wt % of r-GNFs
Epoxy	Pure epoxy matrix	0
N-6/2	Nano-epoxy matrices	0.2
N-6/3		0.3
N-6/5		0.5

The specimens were dried in a vacuum chamber at 60°C for 24 h before the immersion. Each day the weight of specimens were recorded. The weighing was carried out within 30 s to make the error due to evaporation of water negligible. For the UV aging test, another set of matrix specimens were exposed alternately to ultraviolet light for 4 h at 60°C and followed by 4 h of water condensation at 55°C in a UV chamber (model: QUV/SE, Q-Lab Corp.). The wavelength of the UV radiation was 340 nm and the intensity was 0.71 W/m^2. This test was carried out by following ''ASTM G 53-88 Standard Practice for Operating Light and Water Exposure Apparatus (Fluorescent UV-Condensation Type) for Exposure of Nonmetallic Materials.'' As this is our preliminary studies concerning chemical changes in specimens, the exposure time used here is set slightly different from that given in the standards.

Testing

All aged and nonaged matrix specimens were exposed to ambient environment for another 30 days before any FTIR experiments being performed on them. Our purpose is to observe the permanent changes made into the specimens due to hygrothermal and UV expositions. Instant FTIR experiments just after hygrothermal and UV expositions might be influenced by extra moisture content (which can be evaporated if exposed to ambient environment) in the specimens. Step scan photoacoustic FTIR spectra were collected to analyze the changes on surface of specimens due to aging. The experiment was carried out on an IFS66 spectrometer (Brucker Optics Inc.). As both kinds of aging experiments were performed for limited time and chemical changes in specimens due to this ageing effect may be insignificant, utmost care was taken while performing FTIR spectroscopic measurement. The sample compartment of the spectrometer was purged with dry nitrogen gas to eliminate ambient water vapor. IR absorbance spectra were recorded in the range 400–4000 cm^{-1} and the resolution was 4 cm^{-1}. Nonaged, moisture aged and UV aged specimens are abbreviated to Non, M, and UV, respectively, in the following sections.

RESULTS AND DISCUSSION

Moisture absorption

It was found that the rates of water absorption in matrix specimens varied with r-GNF contents. To calculate the rate of water (q) absorption the following equation was used:

$$q = \frac{m_w - m_d}{m_d} \times 100\% \quad (1)$$

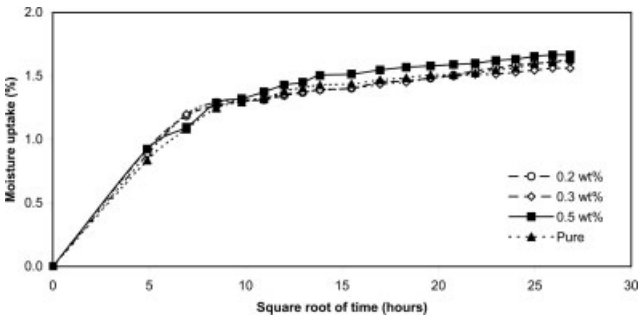

Figure 2 Moisture absorption of matrix specimens with different r-GNF contents.

where m_w and m_d are the masses of the specimen at wet and dry condition, respectively. From Figure 2, it is observed that each matrix specimen absorbed water until the end of the experiment and the absorption process has two stages. In the first stage, fast absorption with time i.e., up to 96 h and moisture absorption is linear with respect to square root of time. The other one is very low rate moisture absorption, which theoretically would not reach to the equilibrium. All the matrices showed similar absorption behavior, which implies that there is no obvious difference in absorption level between the nanoepoxy and pure epoxy matrices. This fact might be attributed to the chemical bonding between nanofibers and epoxy molecules, which is also in agreement with our experimental work on nanoepoxy matrices conducted previously.[29,30]

The moisture absorption behavior of specimens can be explained by Fick's law, which states that moisture absorption (%) with respect to square root of time increases linearly up to a certain time and then slows down and eventually reaches an equilibrium state.[31] The similar kind of analysis was reported in Bagley and Long's work.[32] Bagley and Long considered structural relaxation in this second stage of diffusion. As cured epoxy matrix is in a glassy state, it is reasonable to assume that the relaxation effects are much lower than the diffusion. Therefore, the water absorption rate was uniform through-out the specimens.[32] This means that the first stage was mainly controlled by the diffusion process, whereas the second stage was controlled by the relaxation process.

Generally, an equilibrium point which denotes the maximum moisture absorption, may be observed within a time period of relaxation process. However, in our experiment, after 30 days of moisture absorption, the equilibrium point was not observed. This phenomenon can be clarified by assuming that epoxy, a glassy matrix, would take longer time to attain equilibrium point through relaxation. If the rate of the relaxation process is slower than that of the diffusion, it deviates from Fick's law. Using

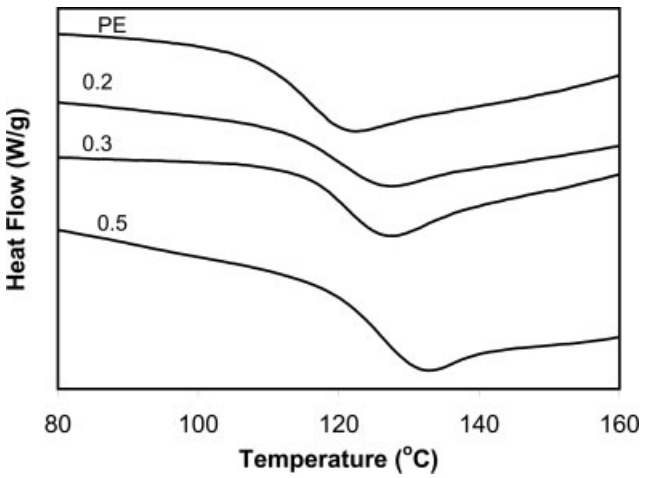

Figure 3 DSC curves of different cured specimens.

periodical thermal spikes, moisture absorption rate can be increased.[33,34] Xiang and Jones[35] found an equilibrium stage in their experiments at high spike temperatures.

DSC behavior

DSC is a thermoanalytical technique in which heat requirement to increase the temperature of a sample can be observed. The principle behind this is that if there is any phase transformation occurs due to temperature change, more (or less) heat will flow to it. It is seen from the Figure 3 that there are peaks in heat flow versus temperature DSC curves of nonaged specimens of all concentrations, which indicates that the specimens were not fully cured. Figure 3 shows the decrease in the peak temperature (T_p) with the increase of r-GNF concentration (Epoxy: 134°C, *N*-6/2: 129°C, *N*-6/3: 128°C and N/6-5: 124°C), which reveals that the addition of the nanofibers lower the curing degree. Similar results were obtained in other nanocomposite systems by other researchers, which provided the explanation for this T_p drop; i.e., the nanofillers may be the preferential adsorption sites of water in the matrix, which leads to nonstoichiometric balance causing the decrease of T_p.[36] In this work, the results of the DSC tests for the nonaged specimens imply that more heat would be needed for nanocomposite curing. The reason is that the r-GNFs also serve as a curing agent for epoxy resins. However, they have a larger molecular size than the curing agent molecules; more heat is required for the overall curing process. These DSC results are in agreement with the studies on the effects of the r-GNFs on curing degree and activation energy of the cure reaction reported in.[23] Generally, resin matrices with lower curing degree would have lower ageing resistance, which is contrary to our previous experimental results of the nanoepoxy matrices. Therefore, it is necessary to explore the ageing mechanisms of the nanoepoxy systems.

FTIR analysis

FTIR analyses were performed to study the changes of molecular conformations of the matrix specimens due to hygrothermal and UV aging. Figure 4 shows the normalized FTIR spectra of the cured nonaged samples of all concentrations. The spectra were normalized with the intensity of the band at 1610 cm^{-1}, which was assigned to the aromatic ring band, for comparison purpose. This band was expected to be stable for all of the samples and was not likely to take part in hygrothermal and UV aging.[37,38] Despite taking utmost care, water noises are shown in the spectra. Moreover, the noise is found in the specimens irrespective of r-GNF concentration and aging conditions. While curing, the epoxide unit of epoxy molecule reacted with both the amine unit in the curing agent and the r-GNF to produce water, which is the source of noise in spectra. The water noise observed in spectra is especially close to carbonyl band, which will be discussed later in details. Several peaks were identified in the Figure 4. The range of FTIR spectra was chosen to be 400–40,000 cm^{-1} and it is observed that the changes occur at the wave numbers 831, 916, 1041, 1105, 1184, 1227, 1580, 1654, 1736, 2930, and 3440 cm^{-1} which may be considered to correspond to different units in matrix as mentioned in Table II.[39–42] The changes of molecular conformation among nonaged specimens of all concentrations can be compared from Figure 4. In FTIR spectra analysis, two parameters (wave number and intensity of absorbance) are considered in this study. While quantifying these two parameters for specimens of different r-GNF concentrations and/or aging conditions, the variations in wave numbers as well as intensity were not observed. However, for

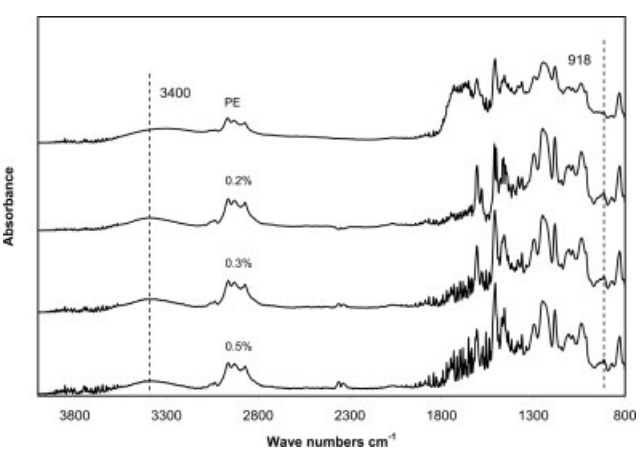

Figure 4 Normalized FTIR spectra of nonaged cured specimens.

TABLE II
Characteristic Bands Related to the Matrix Specimens

Bands (cm^{-1})	Assignment
3440	Hydroxyl (—OH) stretching
3300	N—H stretching
3050	Phenyl—H stretching
2960-2930-2870	Alkyl units (C—H and $-CH_2$) stretching
1725	C=O stretching
1650	O—H bending vibration
1610-1580-1510	Aromatic ring stretching
1450, 1380	C—H in plane deformation in aliphatic units
1290	Twisting mode of $-CH_2-$ units
1250-1170	Stretching of phenyl-C-phenyl, stretching of C—O—C
1034, 1029	Stretching of the trans forms of the ether linkage
916	Epoxy functional unit
824	In plane deformation of phenyl-H

the specimens with the same r-GNF concentration and being aged under the same conditions, the variation in wave numbers was not observed. The intensities among these specimens showed negligible change (up to 2 in three decimal places, e.g., 0.315–0.317).

The curing kinetics depends on several factors such as ingredients, temperature, etc. While curing, the amine reactive unit from both curing agent and r-GNF assist in opening the epoxy ring; as a result, hydroxyl units and secondary amines formed. These secondary amines can react with epoxy rings again and produce tertiary amines and hydroxyl units. Therefore, with more curing, more hydroxyl unit would be produced with the disappearance of the epoxy unit. After curing, both epoxide unit and primary amine peaks should decrease as a result of the amino-epoxy reaction. However, the O—H stretching vibrational bands of water show the complicacy due to intramolecular and intermolecular hydrogen bonding. Both in-plane bending mode and principle stretching vibration occur in the range $\approx$ 3800–2800 cm^{-1}. More complicacies come into play when the spectrum of O—H in water is superimposed by a broad absorption spectrum linked to interaction among OH units in the polymer molecules through hydrogen bonding. Absorption at 3369, 3298, and 3174 cm^{-1} corresponds to the stretching vibration of the primary amine unit ($—NH_2$) of the curing agent. With the reduction of primary amine unit, new absorptions at around 3400 cm^{-1} appear due to formation of hydroxyl (—OH) units and secondary amine (N—H) unit. The little existence of primary amine units tends to be concealed under the —OH band. The existence of a great variety of chemical compounds that assists in making hydrogen bonds broaden the —OH band.

From the spectra shown in Figure 4, it is found that in epoxy specimen, the —OH band broadens more compared to the nanoepoxy matrices with different r-GNF loadings (N/6-2: 0.2 wt %, N/6-3: 0.3 wt %, and N/6-5: 0.5 wt %). From the DSC tests, we found that more curing occurred in epoxy specimens and the order of specimens in their degree of curing is: epoxy > N/6-2 > N/6-3 > N/6-5. Therefore, it validates the results that in epoxy specimens more hydroxyl unit was generated due to more curing compared to that in other specimens. However, N/6-2, N/6-3, N/6-5 cured specimens show little difference in their respective —OH bands. The epoxide unit band at 918 cm^{-1} for epoxy specimen (Fig. 4) confirms the decrease of peak compared with nanoepoxy specimens, which also validates that maximum curing occurred in the pure epoxy specimen.

Comparing the peak positions and the width of water–water hydrogen bonded OH stretching bands in aged and nonaged epoxy specimens [Fig. 5(a)], it is observed that the peak is narrow in moisture-aged (M-aged) and nonaged epoxy specimens, and there is positive shift of the bands (nonaged: 3390, M-aged: 3381 and UV-aged: 3317 cm^{-1}). These bands' positions indicate that hydrogen bonding between water molecules in nonaged and moisture-aged epoxy specimens is weaker compared to those in UV-aged epoxy specimens. The shift of the peaks in the OH stretching band towards higher value occurred due to the interaction between water molecules and the epoxy resin. The weakened water–water hydrogen bonding could assist the water molecules to get rid of epoxy resins as exposed to ambient environment for >1 month. In hygrothermal aging of epoxy specimens, water diffusion took place and the change was not permanent. In presence of UV radiation, further curing took place in epoxy specimens (DSC tests showed that the specimens were not fully cured) with formation of hydroxyl unit, carbonyl unit and reduction of epoxide unit which will be discussed later. The intensity of absorption at —OH band is gradually increasing with aging in this order: nonaged (0.218) < M-aged (0.223) < UV-aged (0.231). Therefore, water absorption in epoxy specimens made the changes in the —OH band domain. Nanoepoxy with r-GNFs [Fig. 5(b) *N*-6/2: 0.2 wt %, (c) *N*-6/3: 0.3 wt % and (d) *N*-6/5: 0.5 wt %] showed same behavior. The peaks for nonaged (3406 cm^{-1}) and M-aged (3400 cm^{-1}) specimens of *N*-6/2 have positive shift compared to that of UV-aged (3309 cm^{-1}) specimens which also has the broadness [Fig. 5(b)]. In Figure 5(c) for the nanoepoxy specimen *N*-6/3 (nonaged: 3380 cm^{-1}, M-aged: 3396 cm^{-1} and UV-aged: 3317 cm^{-1}) and in Figure 5(d) for the nanoepoxy *N*-6/5 (nonaged: 3406 cm^{-1}, M-aged: 3394 cm^{-1} and UV-aged: 3302 cm^{-1}) specimens, we found the same trend, i.e., there are positive shift of

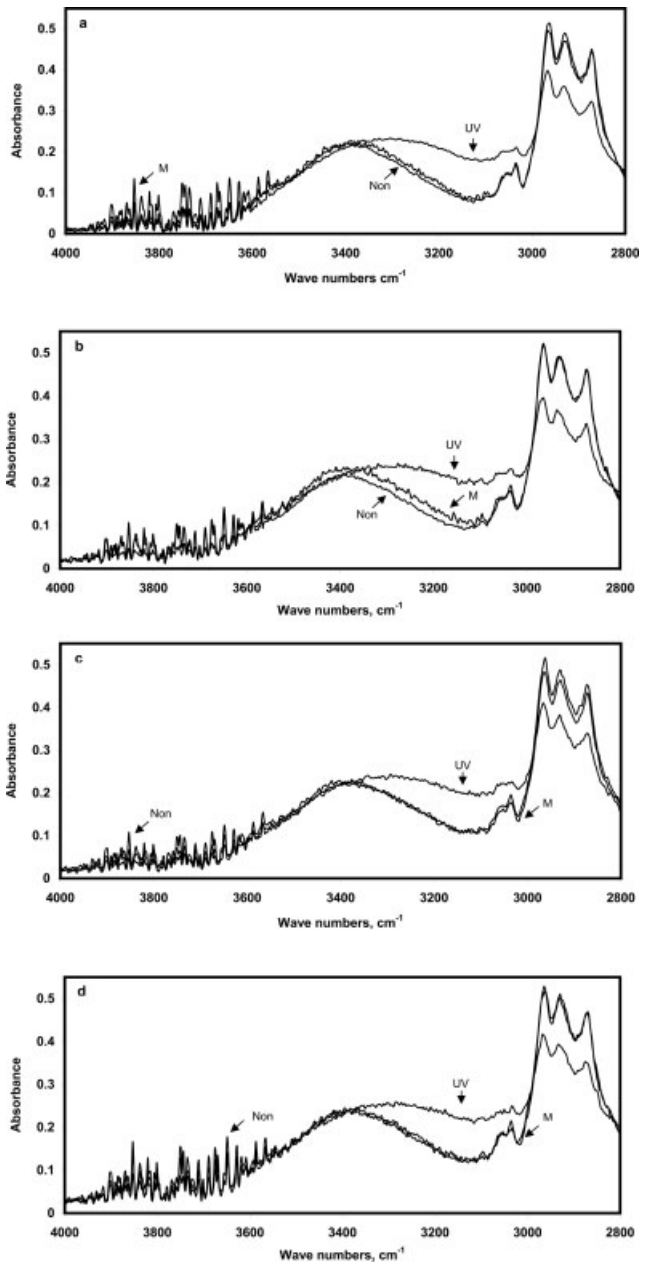

Figure 5 Normalized FTIR spectra of aged and nonaged specimens in band range 2800–4000 cm^{-1}. (a) epoxy, (b) *N*-6/2, (c) *N*-6/3, and (d) *N*-6/5.

OH band in nonaged and M-aged specimens compared to that in UV-aged specimens [Fig. 5(c,d)]. The intensity of absorption at —OH band in r-GNF reinforced specimens shows the same trend as found in epoxy specimens. Comparing the peaks of —OH bands of all kinds of specimens, it is found that more curing and hydroxyl formation occurred due to UV radiation and the order is epoxy < *N*-6/2 < *N*-6/3 < *N*-6/5 and the effect of hygrothermal aging is less compared to UV aging. In the region of 2800–3000 cm^{-1}, it is found that there is decrease in the intensity of band characterizing the disappearance of C—H and —CH_2 stretching in UV specimens of all concentrations. At the presence of UV radiation in humid environment this C—H and CH_2 groups might form the carbonyl groups due to action of oxygen.[43] However, it is observed that with only humid environment these transformations didn't take place as no changes were found at the same region in moisture-aged specimens compared to nonaged specimens.

Beside hydroxyl unit, carbonyl unit shows its presence enormously in the aged specimens, especially in the UV specimens. For the epoxy-amine system, the absorption of these units ranges from 1670 to 1800 cm^{-1} as shown in Figure 6.[44] In the carbonyl region, increment is observed at 1580, 1654, 1675, 1725, and 1736 cm^{-1} and decrement at 1508 and 1458 cm^{-1}. A complex mixture of oxidation products, such as hydroperoxides, alcohols, esters, lactones, ketones, etc. are generated when polymer degradation occurred in the presence of oxygen. However, due to broad range of hydroxyl and carbonyl band, the absorbance peaks of these oxidation products are overlapped with them. From Figure 6(a–d), it is observed that in UV aging, hydrolytic attack is more in all specimens compared to that in hygrothermal aging. Generally under hygrothermal environments, most polymeric materials undergo hydrolysis reaction in presence of ester linkage and the reaction can be expressed as

$$\mathrm{RCOOR'} + \mathrm{H_2O} \leftrightarrow \mathrm{RCOOH} + \mathrm{R'OH} \qquad (2)$$

UV radiation acts as boosting environment to enhance this reaction and generation of carbonyl and hydroxyl units are voluminous compared to that in hygrothermal aging. One of the maxima is obtained at 1734 cm^{-1} and it is found that the intensity of absorption at 1734 cm^{-1} in different types of specimens is different. They are as found, epoxy specimens (UV-aged: 0.917, M-aged: 0.572 and nonaged: 0.315), *N*-6/2 specimens (UV aged: 0.899, M-aged: 0.462 and nonaged: 0.137), *N*-6/3 specimens (UV aged: 0.810, M-aged: 0.284 and nonaged: 0.456), and *N*-6/5 specimens (UV-aged: 0.890, M-aged: 0.580 and nonaged: 0.717). Comparing these intensity values, it can be said that *N*-6/3 specimens show the less absorption at 1734 cm^{-1} and therefore less hydrolytic reaction in *N*-6/3 specimens occurred compared to the other groups. It means less damage in *N*-6/3 specimens compared to other groups. In addition, increases in intensities are observed at 1518, 1592, 1615, 1657, 1675, 1725, and 1739 cm^{-1} and decreases are observed at 1508 and 1458 cm^{-1} in the carbonyl region. The increments at different bands as mentioned above are due to photo-oxidation of different alkyl and phenyl units and formation of different

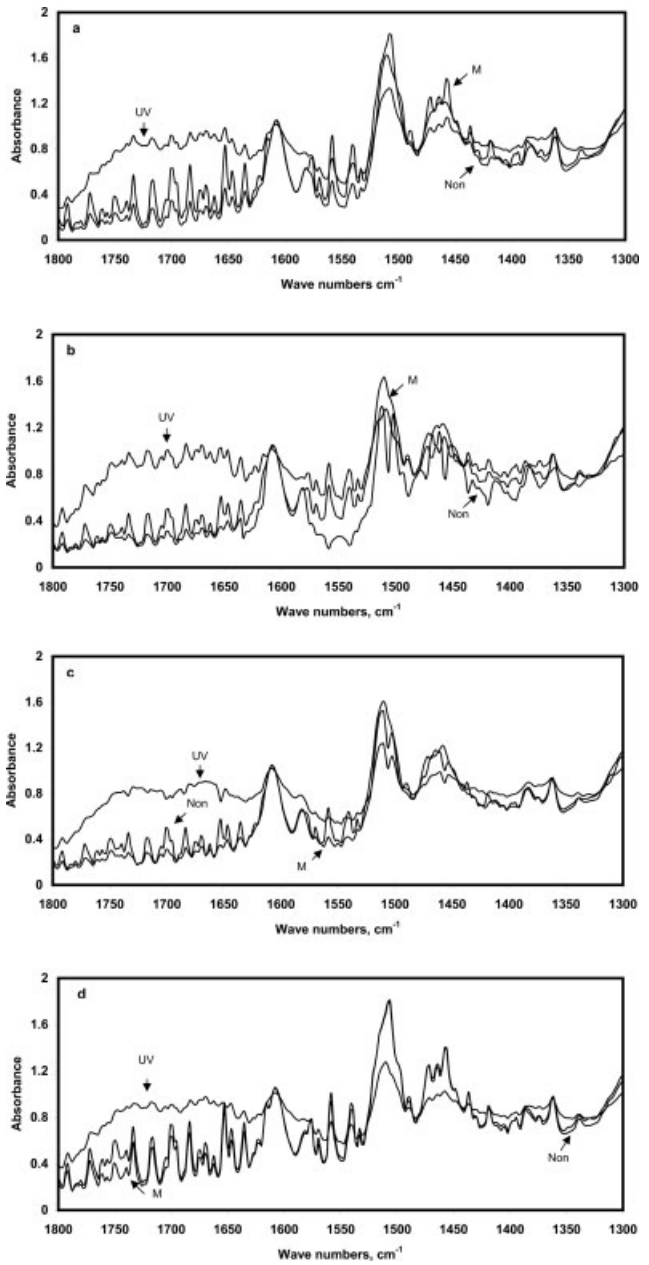

Figure 6 Normalized FTIR spectra of aged and nonaged specimens in band range 1300–1800 cm^{-1}. (a) epoxy, (b) *N*-6/2, (c) *N*-6/3, and (d) *N*-6/5.

carbonyl units. The position of O—H unit at 1650 cm^{-1} (bending vibration) might be concealed by carbonyl bands. The functional groups attached to aromatic rings at 1508 cm^{-1} are significantly modified during irradiation in the presence of oxygen and as a result there is the decrease in the band.

In Figure 7, it is observed that the epoxide unit band at 916 cm^{-1} in all UV-aged specimens of all groups has lower intensity compared to other aged and nonaged specimens in respective group. As mentioned earlier that in presence of UV radiation, further curing can take place and epoxide unit takes part in curing reaction with amine unit producing hydroxyl unit and therefore it validates the occurrence of curing. However, no changes were found in epoxide unit in hygrothermal aging due to hydrolytic degradation as the intensities at 916 cm^{-1} of nonaged and M-aged specimens are same in each group. In addition, there are decreases of intensities at 1250, 1186, 1042, 823 and increase at 1270 cm^{-1}. The photo-oxidation of these groups especially at 1186 cm^{-1} produces the main photoproducts such as acetophenone (1685 cm^{-1}) and benzyl methyl ketone (1734 cm^{-1}).[45]

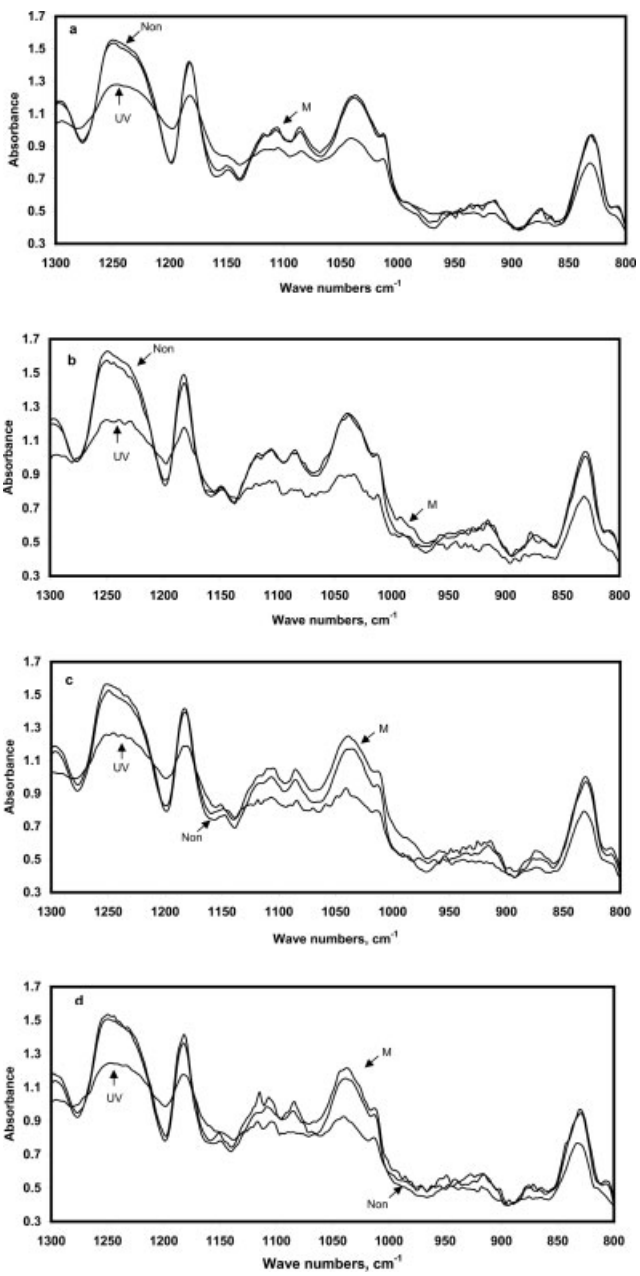

Figure 7 Normalized FTIR spectra of aged and nonaged specimens in band range 800–1300 cm^{-1}. (a) epoxy, (b) *N*-6/2, (c) *N*-6/3, and (d) *N*-6/5.

TABLE III
Different Bands for Different Specimen Groups and Intensities at Corresponding Wave Numbers

		Epoxy			N-6/2			N-6/3			N-6/5		
		Non	M	UV	Non	M	UV	Non	M	UV	Non	M	UV
Hydroxyl unit	Band	3390	3381	3317	3396	3379	3288	3385	3381	3296	3386	3369	3286
	Intensity	0.218	0.223	0.234	0.220	0.232	0.237	0.226	0.217	0.238	0.238	0.244	0.257
Carbonyl unit	Band	1734	1734	1734	1734	1734	1734	1734	1734	1732	1734	1734	1736
	Intensity	0.315	0.572	0.917	0.137	0.462	0.899	0.456	0.284	0.810	0.717	0.580	0.890
Epoxide unit	Band	916	914	916	920	916	916	916	914	914	916	916	918
	Intensity	0.564	0.566	0.486	0.609	0.630	0.486	0.583	0.612	0.475	0.579	0.585	0.507

Non: non-aged, M: hygrothermal-aged, UV: UV-aged.

In the above discussion, the hydroxyl unit, the carbonyl unit and the epoxide unit are considered as main units to judge the behavior of the degradation. In Table III, the wave numbers, intensities at the corresponding wave numbers of different bands for different specimen groups are given. The results may be used to compare the degradations of among different ageing specimens of different groups. The intensities of UV-aged epoxy and *N*-6/3 specimens for epoxide unit are 0.486 and 0.475. The intensities of nonaged E and *N*-6/3 specimens for the epoxide unit are 0.564 and 0.475. Therefore, curing in the *N*-6/3 specimen is much faster compared to curing in the pure epoxy specimen due to the UV radiation. However, the intensities of hydroxyl unit in the UV-aged epoxy and *N*-6/3 specimens are 0.234 and 0.238 and intensities carbonyl unit in UV-aged epoxy and *N*-6/3 specimens are 0.810 and 0.917. Thus, it can be confirmed that the UV radiation did less degradation to the *N*-6/3 specimens compared to the epoxy specimens. Comparing similar kinds of data in M-aged specimen of both E and *N*-6/3 groups, we find that hygrothermal degradation occur less to *N*-6/3 group compared to epoxy groups. UV radiation degrades materials much more compared to hygrothermal expose in our study since the UV conditions are the combination of the humid environment at elevated temperature and UV radiation. Comparing all data in Table III it is found that the order of degradation in terms of groups is like this: epoxy > *N*-6/5 > *N*-6/2 > *N*-6/3, which indicated that the nanoepoxy showed better aging resistance compared to the pure epoxy and the nanoepoxy with 0.3 wt % of r-GNFs is the most effective. This result is in agreement with our previous mechanical test results. The bonding between r-GNF and epoxy molecule possibly works against degradation. However, the resistance of the specimens against the degradation with higher amount of nanofiber such as 0.5 wt % r-GNF was aggravated slightly in comparison to that of specimens with 0.3 wt % r-GNF. This phenomenon can be explained by the effects of higher amount of diluent in the matrix. To remove agglomeration of highly polarized and reactive r-GNF, diluent is necessary. In this study, we used nanoepoxy systems with fixed ratio 1:6 of r-GNF to diluent. For specimens with 0.2 wt % and 0.3 wt % r-GNFs, the amounts of diluent were 1.2 wt % (= 0.2 × 6) and 1.8 wt % (= 0.3 × 6), respectively. The content of diluent increases with the increase of r-GNF wt % and more amount of diluent hinders epoxy crosslinking. Therefore, considering the amounts of epoxy, diluent, r-GNF and their advantages and disadvantages, optimal results was observed in the specimens with 0.3 wt % r-GNF. This preliminary investigation will help in our study on continuous fiber reinforced nanoepoxy matrices, and currently we are applying this nanoepoxy with 0.3 wt % for making various continuous composites; the results of these studies will be reported later.

CONCLUSIONS

Effects of UV radiation and hygrothermal expose on pure epoxy and nanoepoxy matrices were investigated by Fourier Transform infrared spectroscopy (FTIR) analysis. Moisture sorption characteristics of pure epoxy and nanoepoxy matrices in hygrothermal tests show both diffusion and relaxation stages during sorption processes. UV radiation degraded materials much more compared to hygrothermal expose, through analysis of several main groups. First, presence of hydroxyl unit in specimens is enormous. Other unit like carbonyl group is observed due to hydrolysis and photo-oxidation of alkyl, phenyl, and aromatic ether linkage units. The decrease in epoxide group is also observed. It is found that the order of degradation in terms of groups is like this: epoxy > *N*-6/5 > *N*-6/2 > *N*-6/3, which indicates that the nanoepoxy with 0.3 wt % of r-GNFs shows the best ageing resistance, which is in agreement with our mechanical test results. Therefore, this work will certainly assist our further study on continuous fiber reinforced the nanoepoxy matrices.

Dr. W.H. Zhong also gratefully acknowledges Dr. Charles M. Lukehart and Mr. Jiang Li (Vanderbilt University) for providing the derivatized graphitic carbon nanofibers.

References

1. Donnet, J. B. Compos Sci Technol 2003, 63, 1085.
2. Frisch, H. L.; Mark, J. E. Chem Mater 1996, 8, 1735.
3. Jang, B. Z. Advanced Polymer Composites: Principles and Applications; ASM International: Materials Park, OH, 1994.
4. Chand, S. J Mater Sci 2000, 35, 1303.
5. Krumova, M.; Klingshirn, C.; Haupert, F.; Friedrich, K. Compos Sci Technol 2001, 61, 557.
6. Nakajima, K.; Furusawa, M.; Yamamoto, T.; Tashiro, J.; Sasaki, A; Chikyow, T; Ahmet, P; Yamada, H; Yoshimoto, M. Diam Relat Mater 2002, 11, 953.
7. Cooper, C. A.; Young, R. J.; Halsall, M. Compos Part A: Appl Sci Manuf 2001, 32, 401.
8. Chen, G. Z.; Shaffer, M. S. P.; Coleby, D.; Dixon, G.; Zhou, W.; Windle, A. H. Adv Mater 2000, 12, 522.
9. Sandler, J.; Shafter, T. P.; Bauhofer, W.; Schulte, K.; Windle, A. H. Polymer 1999, 40, 5967.
10. Wong, E. W.; Sheehan, P. E.; Lieber, C. M. Science 1997, 277, 1971.
11. Yue, Z. R.; Jiang, W.; Wang, L.; Gardner, S. D.; Pittman, C. U. Carbon 1999, 37, 1785.
12. Li, J.; Vergne, M. J.; Mowles, E. D.; Zhong, W. H.; Hercules, D. M.; Lukehart, C. M. Carbon 2005, 43, 2883.
13. Chen, X. H.; Wang, J. X.; Yang, H. S.; Wu, G. T.; Zhang, X. B.; Li, W. Z. Diam Relat Mater 2001, 10, 2057.
14. Patton, R. D.; Pittman, C. U.; Wang, L.; Hill, J. R. Compos Part A: Appl Sci Manuf 1999, 30, 1081.
15. Carneiro, O. S.; Covas, J. A.; Bernardo, C. A.; Caldeira, G.; Hattum, F. W. J.; Ting, J. M.; Alig, R. L.; Lake, M. L. Compos Sci Technol 1998, 58, 401.
16. Kumar, S.; Doshi, H.; Srinivasarao, M.; Park, J. O.; Schiraldi, D. A. Polymer 2002, 43, 1701.
17. Pervin, F.; Rangaree, V.; Zhou, Y.; Jelanee, S. Proceedings of ASME International Mechanical Engineering Congress, Orlando, Florida, 2005.
18. Pogue, R. T.; Ye, J.; Klosterman, D. A; Glass, A. S.; Chartoff, R. P. Compos: Part A 1998, 29, 1273.
19. Chisholm, N.; Mahfuz, H.; Rangari, V. K.; Ashfaq, A.; Jeelani, S. Compos Struct 2005, 67, 115.
20. Sandler, J.; Werner, P.; Shaffer, M. S. P.; Demchuk, V.; Altstadt, V.; Windle, A. H. Compos: Part A 2002, 33, 1033.
21. Choi, Y.; Sugimoto, K.; Song, S.; Gotoh, Y.; Ohkoshi, Y.; Endo, M. Carbon 2005, 43, 2199.
22. Pan, Y. X.; Yu, Z.; Ou, Y.; Hu, G. J Polym Sci Part B: Polym Phys 2000, 38, 1626.
23. Zhong, W. H.; Li, J.; Xu, L. R.; Lukehart, C. M. Polym Compos 2005, 26, 128.
24. Xiang, Z. D.; Jones, F. R. Compos Sci Technol 1997, 57, 451.
25. Karad, K. S.; Jones, R. F.; Attwood, D. Polymer 2002, 43, 5209.
26. Narisawa, I. Strength of Polymer materials; Khimiya: Moscow, USSR, 1987, p 397.
27. Bursa, J. Proceeding of the Conference Polymer and Structural Composites, Ustron, 1996, 13.
28. Devanne, T.; Bry, A.; Audoin, L.; Verdu, J. Polymer 2005, 46, 229.
29. Neema, S.; Salehi-Khojin, A.; Zhamu, A.; Zhong, W. H.; Jana, S.; Gun, Y. X. J Colloid Interface Sci 2006, 299, 332.
30. Zhamu, A.; Wingert, M.; Jana, S.; Zhong, W. H.; Stone, J. J Compos: Part A 2007, 38, 699.
31. Shen, C. H.; Springer, G. S. J Compos Mater 1976, 10, 2.
32. Bagley, E.; Long, F. A. J Am Chem Soc 1955, 77, 2172.
33. Morgan, R. J.; O'Neal, J. E.; Fanter, D. L. J Mater Sci 1980, 15, 751.
34. McKague, E. L.; Halkias, J. E.; Reynolds, J. D. J Compos Mater 1975, 9, 2.
35. Hough, J. A.; Xiang, Z. D.; Jones, F. R. Key Eng Mater 1998, 144, 27.
36. Miyagawa, H.; Drzal, L. T. Polymer 2004, 45, 5163.
37. Cherdoud-chihani, A.; Mouzali, M.; Abadie, M. J. M. J Appl Polym Sci 1998, 69, 1167.
38. Rockniak, C.; Biernacka, T.; Skarzynski, M. J Appl Polym Sci 1983, 28, 531.
39. Pretsch, E.; Buhlmann, P.; Affolter, C. Structure Determination of Organic Compounds: Tables of Spectral Data; Springer Verlag: Berlin, 2000.
40. Silverstein, R. M.; Webster, F. X. Spectrometric Identification of Organic Compounds, 6th ed.; Wiley: Canada, 1997.
41. Li, Y.; Miranda, J.; Sue, H. J. Polymer 2001, 42, 7791.
42. Han, S. O.; Drzal, L. T. Eur Polym J 2003, 39, 1791.
43. Bellenger, V.; Verdu, J. J App Polym Sci 1985, 30, 363.
44. Delor-Jesin, F.; Drouin, D.; Cheval, P. Y.; Lacoste, J. Polym Degrad Stab 2006, 91, 1247.
45. Rivaton, Polym Degrad Stabil 1995, 49, 11.